

Random-Mass Dirac Fermions in an Imaginary Vector Potential (I): Delocalization Transition and Localization Length

Koujin Takeda*

Institute for Cosmic Ray Research, University of Tokyo, Kashiwa, Chiba, 277-8582 Japan

Ikuo Ichinose†

Department of Electrical and Computer Engineering, Nagoya Institute of Technology, Gokiso, Showa-ku, Nagoya, 466-8555 Japan

In this and subsequent papers, one dimensional system of Dirac fermions with a random-varying mass is studied by the transfer-matrix methods which we developed recently. We investigate the effects of nonlocal correlation of the spatial-varying Dirac mass on the delocalization transition. Especially we numerically calculate both the “typical” and “mean” localization lengths as a function of energy and the correlation length of the random mass. To this end we introduce an imaginary vector potential as suggested by Hatano and Nelson and solve the eigenvalue problem. Numerical calculations are in good agreement with the results of the analytical calculations. We obtain the relation between the localization length of states and the correlation length of the random mass. In subsequent paper, we shall study Dirac fermions with a random mass of long-ranged correlations.

PACS: 72.15.Rn, 73.20.Jc, 72.10.Bg

I. INTRODUCTION

One of the most important problems in condensed matter physics is the localization phenomena in random-disordered systems [1]. At present it is believed that almost all states tend to localize in disorder systems in two and lower dimensions. In some special cases, however, some specific states remain extended even in the presence of strong disorders. System of Dirac fermions with a random-varying mass(RMDF) in one dimension has been studied from this point of view [2–9]. RMDF is a continuum field theory of the random hopping tight binding model and it is related with the random XY spin chain, the random Ising model, polyacetylene system, etc.

In most of studies on the random-disordered systems, only the short-range white-noise random variables are considered. In the previous papers [10–12] we studied the effect of nonlocal correlation of the random mass on the extended states which exist near the band center. For numerical studies, we reformulate the system by transfer-matrix formalism, and obtained eigenvalues and wave functions for various configurations of random telegraphic mass [10]. We verified that the density of states obtained by the transfer-matrix methods is in good agreement with the analytical calculation by supersymmetric methods in Ref. [11]. In this paper we shall introduce an imaginary vector potential into the system of the RMDF and study a localization-delocalization phase transition by varying the magnitude of the vector potential. Through this study we shall obtain the localization length of the states quite accurately as a function of energy and the correlation length of the random mass. This method of calculating the localization length is based on the idea by Hatano and Nelson [13] and it is totally different from the methods which have been used so far [14].

In this and subsequent papers we shall study effects of long-range spatial correlations of the random mass, especially on delocalized states, localization lengths, etc. This work is partially motivated by the recent studies on the one-dimensional Anderson model with random potentials with long-range correlation. There it is shown that there exists a mobility edge at a finite energy if the correlation is long-range enough. As we explained above, extended states exist at the band center in the present model even for the white-noise random mass. Then it is interesting to see if additional extended states appear as a result of the long-range correlation of the random mass.

This paper is organized as follows. In Sec.2, we first explain the imaginary-vector potential methods(IVPM) for calculating the typical and mean localization lengths. Then we compare numerical results with the analytic calculations in order to verify the validity of the IVPM. In Sec.3, we shall consider the system of the RMDF in which a Gaussian distribution is employed for distances between (anti-)kinks or jumps of the telegraphic random mass. We calculate the correlation length of the random mass and also the localization lengths as a function of the mean distance and standard deviation. Then we obtain relation between the correlation length of the random mass and the localization lengths. Section 4 is devoted to conclusion.

The studies on the Anderson model etc., in one dimension employ specific techniques like the Hamiltonian mapping, the renormalization group, etc. Compared with them, our method are rather straightforward. Before calculating the localization lengths, we obtain landscapes of the wave functions which are useful to get physical pictures of the delocalization transition.

II. MODEL, TMM AND IVPM

We shall consider a Dirac fermion in one spatial dimension with a coordinate-dependent mass $m(x)$ and in an imaginary vector potential g , whose Hamiltonian is given by,

$$\mathcal{H} = \int dx \psi^\dagger h \psi, \quad (1)$$

$$h = -i\sigma^z(\partial_x + g) + m(x)\sigma^y, \quad (2)$$

where $\vec{\sigma}$ are the Pauli matrices. This fermion model is a low-energy effective model of random-hopping tight binding models, random-bond spin chains, etc [5]. We introduce the components of ψ as $\psi = (u, v)$. In terms of them the Dirac equation is given as,

$$\begin{aligned} \left(\frac{d}{dx} + g + m(x) \right) u(x) &= Ev(x), \\ \left(-\frac{d}{dx} - g + m(x) \right) v(x) &= Eu(x). \end{aligned} \quad (3)$$

(We follow the notations in Ref. [3].) From Eqs.(3), we obtain the Schrödinger equations,

$$\begin{aligned} \left(-\frac{d^2}{dx^2} - 2g\frac{d}{dx} - m'(x) + (m^2(x) - g^2) \right) u(x) \\ = E^2 u(x), \end{aligned} \quad (4)$$

and similarly for $v(x)$.

In this paper we restrict the shapes of $m(x)$ to multi-kink-anti-kink configurations [15]. The multi-soliton-antisoliton configurations are given by,

$$\begin{aligned} m(x) = \sum_i \bar{m}(\theta(x - \alpha_i) - 1) \\ + \sum_j \bar{m}(\theta(-x + \beta_j) - 1), \end{aligned} \quad (5)$$

where α_i 's(β_j 's) are positions of kinks(anti-kinks) and they are random variables in the present system. An example of $m(x)$ is given in Fig.1.

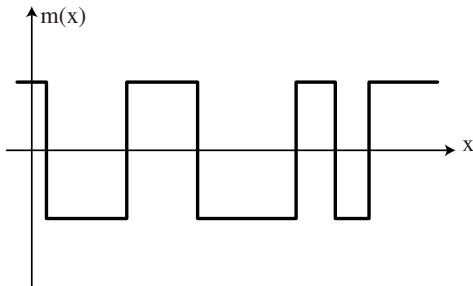


FIG. 1. An example of configurations of solitons and anti-solitons.

If we vary the distances l between soliton and anti-soliton according to the exponential distribution like,

$$P(l) = \frac{1}{2\tilde{\lambda}} \exp\left(-\frac{l}{2\tilde{\lambda}}\right), \quad (6)$$

where $\tilde{\lambda}$ is a parameter, then $m(x)$ has the following correlation [3],

$$[m(x) m(y)]_{\text{ens}} = \frac{A}{\tilde{\lambda}} \exp(-|x - y|/\tilde{\lambda}), \quad (7)$$

where $\sqrt{\frac{A}{\tilde{\lambda}}}$ essentially corresponds to the height of the soliton and anti-soliton, i.e., \bar{m} in (5). From (7), $\tilde{\lambda}$ is the correlation length of the random mass and the limit $\tilde{\lambda} \rightarrow 0$ corresponds to the white-noise case. In the subsequent papers [16,17], we shall study Dirac fermions with long-range correlated random mass by using the methods examined in this paper. There we expect some interesting phenomena like existence of nontrivial mobility edge, nonuniversality of the multi-fractal exponents, etc. Studies in this section show that the IVPM for calculating the localization lengths are reliable and we shall use them for studies on random systems with long-range correlated disorder.

For the vanishing imaginary vector potential, we can solve the Schrödinger equations in (4) under the periodic boundary condition with various multi-soliton-antisoliton configurations of $m(x)$ using the transfer-matrix method(TMM). We can also obtain the energy spectrum and wave functions [10] using this method.

We review the TMM method briefly. Let us consider the Dirac equation (3) with a mass configuration which has a kink at $x = 0$,

$$m(x) = \bar{m}(2\theta(-x) - 1) + m_0, \quad (8)$$

where $\theta(x)$ is the Heaviside function,

$$\theta(x) = \begin{cases} 0 & (x < 0) \\ 1 & (x > 0) \end{cases}, \quad (9)$$

and it is assumed that

$$\bar{m} > m_0 > 0.$$

Substituting (8) into (4), we obtain a Schrödinger equation with a potential which is a combination of the delta function and the step function,

$$\begin{aligned} V(x) = \mp m'(x) + m^2(x) = \pm 2\bar{m}\delta(x) + 4m_0\bar{m}\theta(-x) \\ + (\bar{m} - m_0)^2. \end{aligned} \quad (10)$$

For such a field equation with a delta-function-type potential, the continuity of the wavefunction $u(x)$ leads automatically to the conditions on its derivative $u'(x)$. For example, if we rewrite the Schrödinger equation as

$$\left(-\frac{d^2}{dx^2} + 2\bar{m} \delta(x) + 4m_0\bar{m} \theta(-x)\right) u(x) = (E^2 - (\bar{m} - m_0)^2) u(x), \quad (11)$$

(here we restrict g to zero) and integrate Eq.(11) with respect to x in the range $-\epsilon \leq x \leq \epsilon$, we have

$$\begin{aligned} & -u'(0+\epsilon) + u'(0-\epsilon) + 2\bar{m} u(0) + 4m_0\bar{m} \int_{-\epsilon}^0 dx u(x) \\ & = (E^2 - (\bar{m} - m_0)^2) \int_{-\epsilon}^{\epsilon} dx u(x). \end{aligned} \quad (12)$$

We see the *r.h.s.* of Eq.(12) vanishes in the limit $\epsilon \rightarrow 0$ due to the continuity of $u(x)$. A similar argument applies to $v(x)$ and we have conditions,

$$\begin{aligned} u'(0+0) - u'(0-0) &= 2\bar{m}u(0), \\ v'(0+0) - v'(0-0) &= -2\bar{m}v(0). \end{aligned} \quad (13)$$

We look for solutions under these conditions.

Let the energy eigenvalue E satisfy

$$\bar{m} - m_0 > E > 0, \quad (14)$$

then $u(x)$ takes the form,

$$u(x) = \begin{cases} A e^{\kappa_1 x} + B e^{-\kappa_1 x} & (x < 0), \\ C e^{\kappa_2 x} + D e^{-\kappa_2 x} & (x > 0), \end{cases} \quad (15)$$

$$\kappa_1 = \sqrt{(\bar{m} + m_0)^2 - E^2}, \quad (16)$$

$$\kappa_2 = \sqrt{(\bar{m} - m_0)^2 - E^2}. \quad (17)$$

From the continuity of $u(x)$,

$$A + B = C + D, \quad (18)$$

and Eq.(13) gives

$$\kappa_2(C - D) - \kappa_1(A - B) = 2\bar{m}(A + B). \quad (19)$$

Hence,

$$u(x) = A e^{\kappa_1 x} + B e^{-\kappa_1 x}, \quad \text{for } x < 0 \quad (20)$$

and for $x > 0$,

$$\begin{aligned} u(x) &= \left[\frac{2\bar{m} + \kappa_1 + \kappa_2}{2\kappa_2} A + \frac{2\bar{m} - \kappa_1 + \kappa_2}{2\kappa_2} B \right] e^{\kappa_2 x} \\ &+ \left[\frac{-2\bar{m} - \kappa_1 + \kappa_2}{2\kappa_2} A + \frac{-2\bar{m} + \kappa_1 + \kappa_2}{2\kappa_2} B \right] e^{-\kappa_2 x}. \end{aligned} \quad (21)$$

If we let $m_0 = 0$, $\kappa_1 = \kappa_2 \equiv \kappa$, Eq.(21) simplifies to

$$u(x) = \begin{cases} A e^{\kappa x} + B e^{-\kappa x}, & (x < 0) \\ \left[\frac{\bar{m} + \kappa}{\kappa} A + \frac{\bar{m}}{\kappa} B \right] e^{\kappa x} \\ + \left[-\frac{\bar{m}}{\kappa} A + \frac{-\bar{m} + \kappa}{\kappa} B \right] e^{-\kappa x}. & (x > 0) \end{cases} \quad (22)$$

Values of A , B and E are determined by boundary conditions, *e.g.*, $u(-L/2) = u(L/2) = 0$ for a given system size L .

We restrict m_0 to zero in the rest of the discussion. Since the wavefunction $u(x)$ is expressed everywhere as

$$u(x) = A e^{\kappa x} + B e^{-\kappa x}, \quad (23)$$

we can represent the eigenfunction in terms of coefficients A and B . By using matrix representation and from (21), the conditions (13) give the following relation between the coefficients A and B ,

$$\begin{aligned} \begin{pmatrix} A(x > 0) \\ B(x > 0) \end{pmatrix} &= T \begin{pmatrix} A(x < 0) \\ B(x < 0) \end{pmatrix}, \\ T &= \begin{pmatrix} 1 + \frac{\bar{m}}{\kappa} & \frac{\bar{m}}{\kappa} \\ -\frac{\bar{m}}{\kappa} & 1 - \frac{\bar{m}}{\kappa} \end{pmatrix}. \end{aligned} \quad (24)$$

For kink instead of anti-kink, we should replace \bar{m} with $(-\bar{m})$ in Eq.(24) and we obtain

$$\begin{pmatrix} A(x > 0) \\ B(x > 0) \end{pmatrix} = T^{-1} \begin{pmatrix} A(x < 0) \\ B(x < 0) \end{pmatrix}. \quad (25)$$

Let us define

$$\begin{aligned} R(\kappa, a) &\equiv \begin{pmatrix} e^{\kappa a} & 0 \\ 0 & e^{-\kappa a} \end{pmatrix}, \\ \phi &\equiv \frac{\bar{m}}{\kappa}, \end{aligned} \quad (26)$$

and TM for the configuration of an anti-kink and a kink is given by

$$\begin{aligned} & R(b)T^{-1}R(a)T \\ &= R(b) \begin{pmatrix} e^{\kappa a} - 2\phi^2 \sinh \kappa a & 2\phi(1 - \phi) \sinh \kappa a \\ 2\phi(1 + \phi) \sinh \kappa a & e^{-\kappa a} + 2\phi^2 \sinh \kappa a \end{pmatrix} \\ &\equiv T(a, b), \end{aligned} \quad (27)$$

where a is the distance between the kink and anti-kink.

We impose *periodic* boundary condition on the wavefunction. The above argument can be generalized to an arbitrary number of kink and anti-kink pairs readily and we have the following equation expressed by the transfer matrices.

$$\det \left[T(e, f) \cdots T(c, d)T(a, b) - \begin{pmatrix} 1 & 0 \\ 0 & 1 \end{pmatrix} \right] = 0. \quad (28)$$

We are not able to solve (28) analytically for arbitrary configuration of pairs of kinks. However it is not so difficult to solve it numerically. We can also easily obtain eigenfunctions after having energy eigenvalues by using TM method. It is straightforward to extend the above formalism for nonvanishing m_0 .

Let us introduce the constant imaginary vector potential g . Effect of the imaginary vector potential was discussed by Hatano and Nelson [13]. Let us denote the eigenfunction of energy E for $g = 0$ as $\Psi_0(x)$, and suppose the shape of $\Psi_0(x)$ as

$$\Psi_0(x) \cong \exp\left(-\frac{|x - x_c|}{\xi_0}\right), \quad (29)$$

where ξ_0 is the localization length and x_c is the center of this localized state. When we turn on the constant imaginary vector potential g , the eigenfunction is obtained from $\Psi_0(x)$ by the ‘‘imaginary’’ gauge transformation,

$$\Psi(x) \cong \exp\left(-\frac{|x - x_c|}{\xi_0} - g(x - x_c)\right). \quad (30)$$

This means that the localization length of this eigenfunction is

$$\begin{aligned} \xi_g &= \frac{\xi_0}{1 + g\xi_0} \quad (x > x_c) \\ \xi_g &= \frac{\xi_0}{1 - g\xi_0} \quad (x < x_c). \end{aligned} \quad (31)$$

At the point $g = 1/\xi_0$, the localization length for $x < x_c$ diverges. If the imaginary vector potential g gets larger than this value, ξ_g for $x < x_c$ becomes negative, and the eigenfunction cannot exist at the same energy since it cannot satisfy periodic boundary condition (Fig.2).

So if localized eigenstate with energy E disappears at $g = g_c$ as g is increased, then the localization length of the eigenstate $\Psi_0(x)$ is $1/g_c$. Actually it is shown that for $g > g_c$, energy eigenvalue of the state has an imaginary part and the state is extended as we shall see shortly [13].

The TMM can be easily extended for the case of nonvanishing g . We obtain energy eigenvalues and eigenfunctions numerically. In actual calculation the system size is finite, and the energy eigenvalues of the wavefunctions for $g = 0$ and $g \neq 0$ are slightly different as we mentioned above. We must trace the changes of energy eigenvalues of states for nonzero g on the two dimensional ($E - g$) plane and find the end point of the locus (Fig.3).

In the numerical calculation, we first find the energy eigenstate for $g = 0$. We denote its energy eigenvalue as E_0 . Then we increase g and search the eigenstate in the region $E_0 - \delta E < E < E_0 + \delta E$. (We set δE very small.) Let us suppose that the eigenstate vanishes in this energy region at the value $g = g_1$. We denote the energy eigenvalue of the eigenstate for $g = g_1$ as E_{g_1} . We change the energy region for searching eigenstate as $E_{g_1} - \delta E < E < E_{g_1} + \delta E$ and let g larger than g_1 . We repeat this procedure. If we cannot find energy eigenvalue at the value g larger than g_c , we judge that the localization length of the eigenstate for $g = 0$ is $1/g_c$.

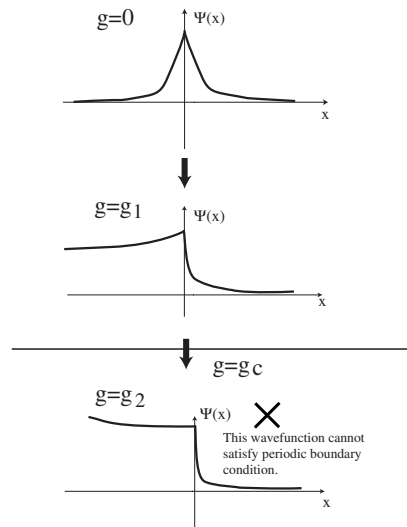


FIG. 2. The imaginary vector potential method

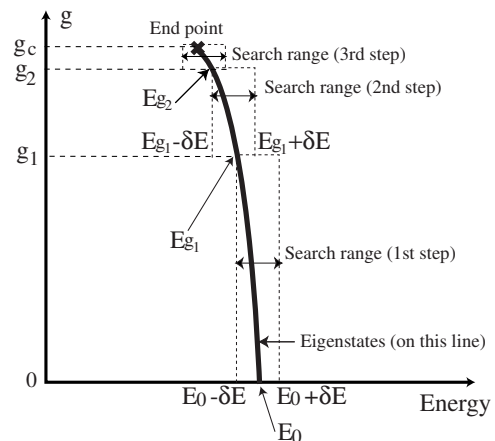


FIG. 3. The procedure of imaginary vector potential method in the numerical calculation

First of all, we show that the delocalization transition actually occurs at finite g . In Fig.4, we show the wave functions of a low-lying state in vanishing and nonvanishing imaginary vector potential. For $g = 0$, the state is obviously localized whereas at $g = 0.03$ the state becomes extended and the energy eigenvalue has an imaginary part. As discussed in Ref. [13], the density distribution of a particle is given by $|\Psi(x, -g)\Psi(x, g)|$ where $\Psi(x, -g)$ is equal to the left eigenfunction.

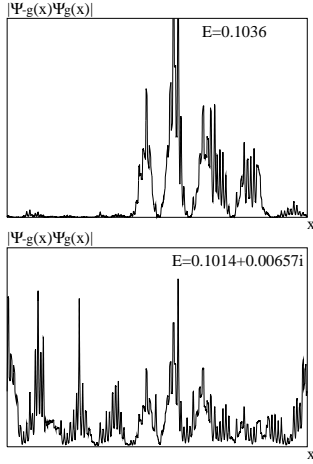


FIG. 4. An example of the localized and the extended wave functions in vanishing and nonvanishing imaginary vector potential $g = 0$ and $g = 0.03$. The state of $g = 0.03$ has a complex energy eigenvalue.

Let us turn to the localization length. For the white-noise case $[m(x)m(y)]_{ens} = A \delta(x - y)$, “typical” localization length or the inverse of the Lyapunov exponent was obtained as [3,18,19]

$$\xi_t(E) = |\ln E/2A|. \quad (32)$$

Numerically the typical localization length $\xi_t(E)$ is obtained by averaging over localization lengths of *all* eigenstates with energy E . On the other hand, Balents and Fisher calculated the averaged Green function and obtained the mean localization length from the spatial decay of the Green function [5]. The result is

$$\xi_m(E) = |\ln E/2A|^2. \quad (33)$$

Case of nonlocally correlated random mass was studied in Refs. [11,12] and $\xi_m(E)$ is obtained as a function of $\tilde{\lambda}$ in Eq.(7).

By numerical calculation we obtain both the typical and mean localization lengths. As we mentioned above, the typical localization length is the average over all solutions of the Schrödinger equation (4), whereas the mean localization length is determined by the states which make dominant contributions to the Green function, i.e., which have large localization length.

The result of the numerical calculation of the typical localization length of the white-noise case is given in Fig.5. We show the ratio of the numerical results to the analytical expression in Eq.(32) in order to compare these two results. Therefore if the energy dependences of the localization lengths obtained numerically and analytically are the same, this ratio should be constant. In Fig.5, the ratio seems constant over the whole range of E .

In Fig.6, we show the numerical results of the “mean” localization length. Here we use the solutions to the

Schrödinger equation which have long localization length. More precisely, “large” localization length ξ means the one which satisfies $\xi > (\text{the “typical” localization length}) + 1.0 \sigma$ in each energy slice. From Fig.6, we conclude that the energy dependence of the mean localization length obtained numerically is in agreement with Eq.(33).

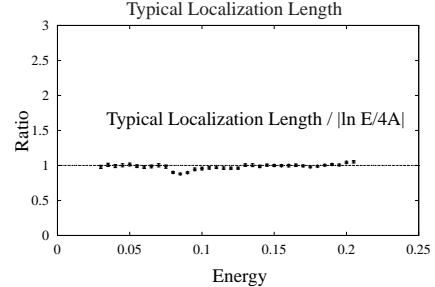


FIG. 5. The comparison between the analytical and the numerical results of the typical localization length for the (almost) white-noise case, *i.e.*, small- λ case: In the numerical calculation, we set $L(\text{system size}) = 50$, $A = 1/2$, $\lambda = 1/60$ in Eq.(7), and the energy slice $\Delta E = 0.01$. The ratio is normalized at $E = 0.15$, and this result is averaged over about 15000 eigenstates. The analytical and the numerical results are in good agreement.

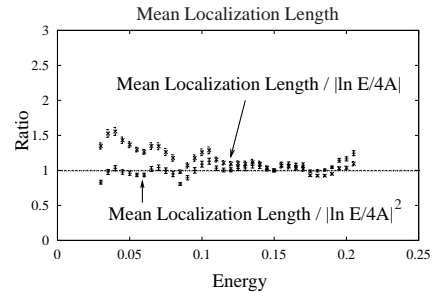


FIG. 6. The comparison between the analytical and the numerical results of the mean localization length: Here we picked up the eigenstates which have large localization length. (See the text.) We show the ratios of the numerical calculation both to Eqs.(32) and (33). We set $L = 50$, $A = 1/2$ and the energy slice $\Delta E = 0.02$. The ratios are normalized at $E = 0.15$.

We shall turn to the case of the nonlocally-correlated disorder. In the white-noise limit ($\tilde{\lambda} = 0$ case in Eq.(7)), the localization lengths diverge only at $E = 0$, that is, extended states exist only at $E = 0$. If we let $\tilde{\lambda} > 0$, the random mass becomes nonlocally-correlated, and the critical energy or the mobility edge at which the delocalization transition occurs may change.

We investigate the “typical” and “mean” localization lengths in the case of nonvanishing $\tilde{\lambda}$ ’s. The behaviour of the “typical” and “mean” localization lengths obtained as

in the white-noise case are given in Figs.7 and 8. It seems that there is *no* $\tilde{\lambda}$ -dependence in the typical localization length. On the other hand, Fig.8 shows that the mean localization length has a small but finite dependence on $\tilde{\lambda}$.

From the above calculations, we conclude that the effect of the short-range correlations in disorders is not so large. Especially the result indicates that the delocalization transition occurs at $E < 0.03$. (If the mobility edge exists at $E_c > 0$, the ratio in Fig.7 or 8 must diverge at E_c .) The delocalization transition probably occurs at $E = 0$.

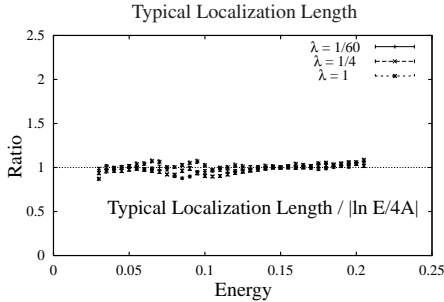


FIG. 7. The behaviour of the localization length in the case of nonvanishing λ 's: Here we show the ratios of the typical localization lengths to $|\ln E/4A|$ (Eq.(32)). We set $L = 50$, $A = 1/2$ and the energy slice $\Delta E = 0.01$. The ratio is normalized at $E = 0.15$.

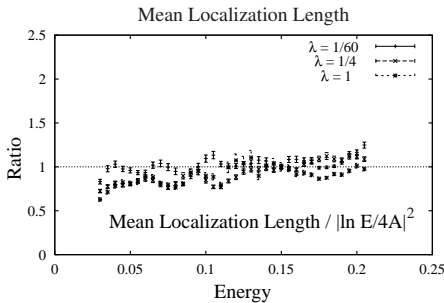


FIG. 8. The behaviour of the localization length in the case of nonvanishing λ 's: We show the ratios of the mean localization lengths to $|\ln E/4A|^2$ (Eq.(33)). We set $L = 50$, $A = 1/2$ and the energy slice $\Delta E = 0.02$. The ratio is normalized at $E = 0.15$.

In the previous paper [12] we calculated the localization length for the random mass with the short-range correlation (7). We obtained the “mean” localization length to the 1st order of $\tilde{\lambda}$ by means of the Green function method. The result is

$$\xi(E) = \frac{1}{A} \left(\frac{\ln \left| \frac{E}{2A} \right|^2}{\pi^2} + A\tilde{\lambda} \frac{4 \left| \ln \frac{E}{2A} \right|}{\pi^2} \right) + O(\tilde{\lambda}^2). \quad (34)$$

In Fig.9 we show the ratios of the numerical result to the analytical calculation up to the 0th and the 1st order of $\tilde{\lambda}$.

This shows that the analytical result with the 1st order correction of $\tilde{\lambda}$ is in better agreement with the numerical result, but the correction is small.

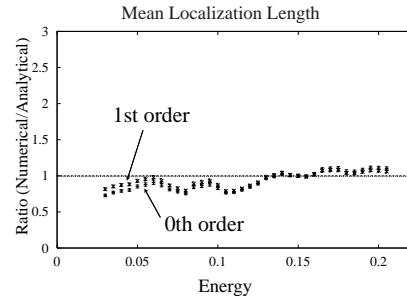


FIG. 9. The comparison between the numerical result and the analytical one in the case of relatively large λ : We show the ratios of the mean localization length calculated numerically to the ones obtained analytically (Eq.(34)). Here we used the analytical results of the 0th and the 1st order of λ . We set $\lambda = 1/4$, $A = 1/2$ and $L = 50$. The energy slice is $\Delta E = 0.02$, and the ratio is normalized at $E = 0.15$.

From the investigations given as far we can conclude that the numerical methods used in this paper are reliable for calculating the localization lengths. It is very interesting to study the case of disorders with a long-range correlation. We expect that a nontrivial mobility edge $E_c > 0$ exists for a certain long-range correlated random mass. Actually the one-dimensional Anderson model with long-range correlated disorder was studied [20], and it is shown that there exists a nontrivial mobility edge.

We can also calculate exponents of the multi-fractal scaling [21] by the TMM [10]. These problems are under study and results will be reported in a future publication [17].

III. GAUSSIAN-DISTRIBUTED DISTANCES BETWEEN KINKS: CORRELATION LENGTH VS. LOCALIZATION LENGTHS

In subsequent papers [16,17] we shall study the localization length with long-range correlated disorder with the TMM and IVP. Before that study, we shall consider the case of Gaussian distribution for distances between kinks in this section. That is, the probability distribution function P_G for distance l is given by the Gaussian distribution,

$$P_G(l) = \frac{1}{\sqrt{2\pi}\sigma} \exp\left\{-\frac{(l - \mu)^2}{2\sigma^2}\right\}, \quad (35)$$

where μ is the mean distance and σ is the standard deviation. If σ is small, eigenstates at low energy (eigenstates

which have a small number of nodes) spread over whole system, and a mobility edge may exist at a nonzero energy. Physically, the mean distance corresponds to the kink density (it can be viewed as impurity density in the related models such as the random hopping tight binding model, spin chain, etc.) and standard deviation controls the degree of randomness. This is in sharp contrast to $P(l)$ in Eq.(6) in which only one parameter $\tilde{\lambda}$ exists.

We first show the relation between localization lengths of eigenstates and the deviation σ . The result is shown in Fig.10. There are several peaks of localization length in these figures with small σ . We know that the energy spectrum is discrete and all states become extended in the case of periodic $m(x)$, i.e., the limit $\sigma \rightarrow 0$, as dictated by the Bloch theorem. For small but finite σ , we expect that energy spectrum is not discrete and eigenvalues spread within narrow energy band. We also expect that localization lengths of states are very large, but finite for nonvanishing σ .

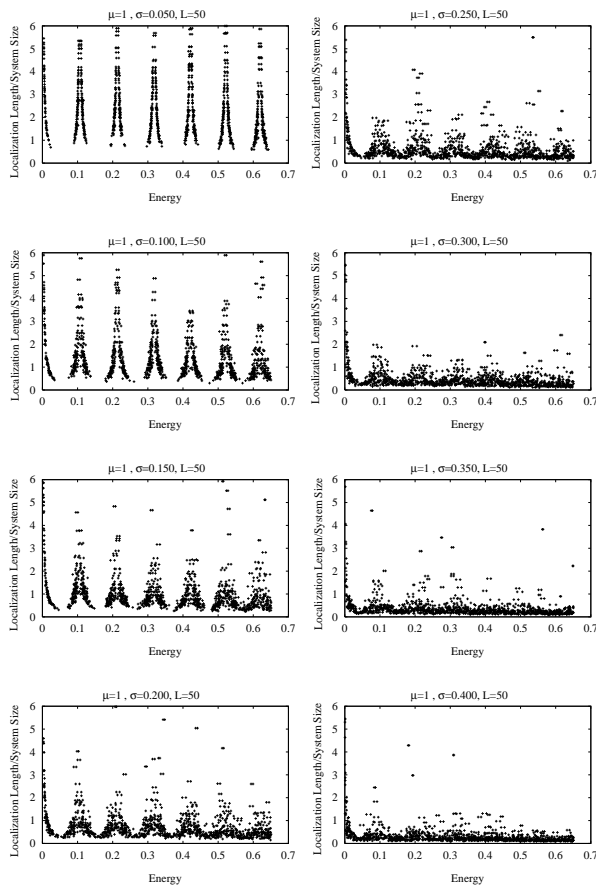


FIG. 10. Localization length and standard deviation of Gaussian distribution: Here we set $L(\text{system size})=50$. In the case of small σ , the points concentrate around the eigenvalues of periodic system and they form several peaks. As we let σ larger, the peaks disappear and these figures become similar to the one in case of white-noise disorder. (Extended state exists only at $E=0$ and other states localize.)

In a system of *finite size*, we regard state as extended one if the localization length is larger than the system size. We can see that localization lengths of several states become larger than the system size if we take σ small. This means that some eigenstates become extended in finite size system.

If we let σ much larger, these peaks of localization length get smaller and disappear except for the one at $E=0$. We recall that the state at $E=0$ is “isolated” extended state in the system with white-noise correlated random mass. In the case of large σ , the random mass $m(x)$ becomes short-ranged and therefore all states except those close to $E=0$ tend to localize.

Next we show the two-point correlation function of random mass $[m(x)m(0)]_{\text{ens}}$ (Fig.11). It oscillates due to Gaussian distributed randomness. The period of this oscillation reflects mean value of Gaussian distribution. The value of envelope of $[m(x)m(0)]_{\text{ens}}$ approaches to zero for larger x , and the envelope shows exponential decay, as we can see in Fig.11. This behaviour is the same as in the case of exponentially distributed kink distances. In the present case, however, we can obtain the system with long-range correlated disorder in which there are a *large* number of kinks. (In the case of exponential distribution $P(l)$ in Eq.(6), there are a small number of kinks in the system with large correlation length, and the distribution with $P(l)$ is not sufficient for studies on practical systems like random spin chains.) The correlation length of random mass is very large and exceeds system size for small σ .

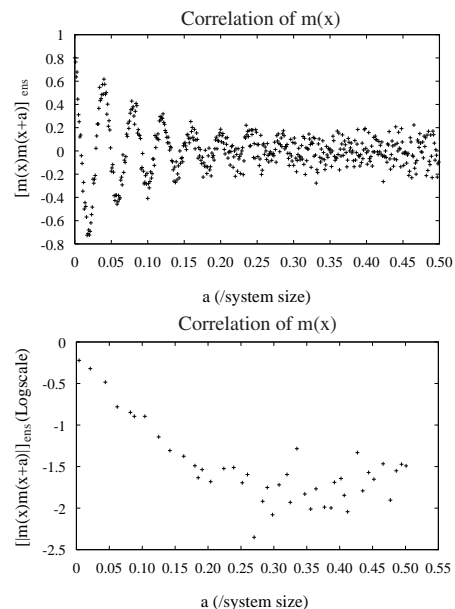


FIG. 11. Correlation of random mass with Gaussian distributed randomness: Here we set $\mu=1$, $\sigma=0.20$ and $L(\text{system size})=50$. We show the behaviour of envelope in the logscale plot. From this figure, we know that $m(x)$ is exponentially correlated in this case.

The relation between σ and the correlation length λ (decay rate) of random mass is shown in Figs.12 and 13. (λ is defined from the envelope of correlation of $m(x)$ as $[m(x)m(x+a)]_{\text{ens}} \sim \exp(-a/\lambda)$.) From Fig.13, we conclude that these quantities are related as

$$\lambda = A\sigma^{-\nu}. \quad (36)$$

In the case shown in Fig.13, A and ν are estimated as

$$\begin{aligned} A &= 4.91 \times 10^{-3}, \nu = 1.881 \quad (L = 50, \mu = 1), \\ A &= 2.67 \times 10^{-3}, \nu = 1.837 \quad (L = 100, \mu = 1), \end{aligned} \quad (37)$$

where L is the system size.

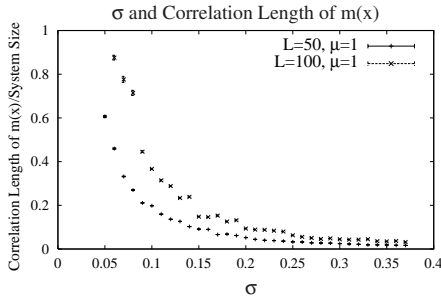


FIG. 12. Relation between deviation σ of Gaussian distribution and correlation length λ of random mass(1): λ is defined as $[m(x)m(x+a)]_{\text{ens}} \sim \exp(-a/\lambda)$. In the case of small σ , correlation length of $m(x)$ is much larger than the system size.

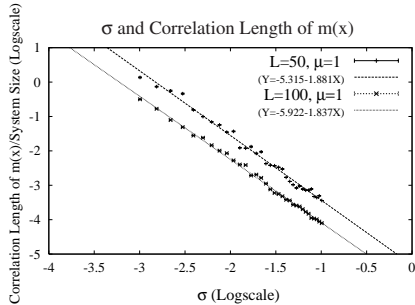


FIG. 13. Relation between deviation σ of Gaussian distribution and correlation length λ of random mass(2) (Logscale *vs.* logscale plot): Points for fixed system size are almost on one line.

We observe the typical localization length of the states at a fixed energy and also its dependence on system size. We have already seen that energy eigenvalues of the states concentrate around several energy values. In order to calculate typical localization length, we pick up the states around second peak from the lowest energy and average localization lengths of these states. (See Fig.10. In the actual calculation, we picked up the states around $E \simeq 0.1$ in the system with $L = 50$, $\mu = 1$, and the

ones around half(quarter) of this energy value in the double(four times) size system.)

The dependences of typical localization length on σ and system size are shown in Fig.14. We expect that the σ dependence of localization length ξ can be fit by following function,

$$\xi = A |\sigma - \sigma_c|^{-\eta}, \quad (38)$$

where σ_c is critical value and η is critical exponent. Strictly speaking, this relation holds true only in infinite size system. We expect that we can assume this parameterization if the system size is large enough.

The result of fitting is shown in the Table 1. We conclude that the choice of this fitting function is valid from these χ^2 values and also from the fact that the critical exponents for different system sizes are almost the same.

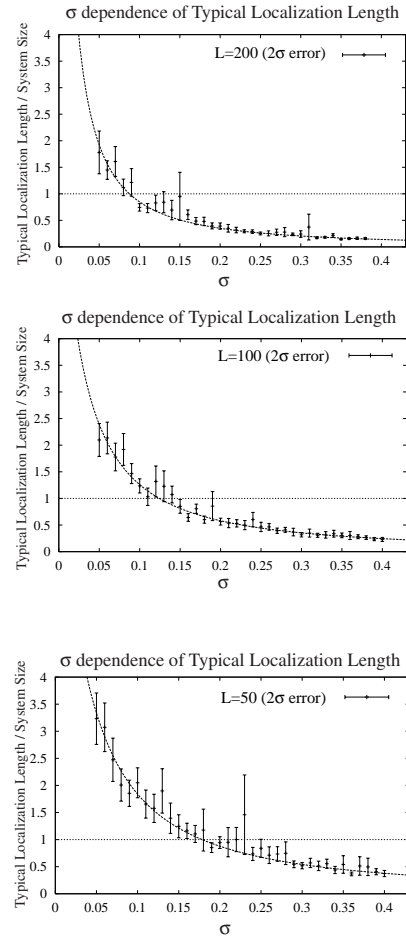


FIG. 14. Typical localization length and deviation σ : We see the σ dependences of typical localization lengths for second peak in various size systems. Here we set μ (mean distance)= 1. We also show the results of fitting. (They are shown as the curve in each figure.)

Table 1

| L | $A(\times 10^{-2})$ | $\sigma_c(\times 10^{-2})$ | η | $\frac{\chi^2}{\text{freedom}}$ |
|-----|---------------------|----------------------------|-------------------|---------------------------------|
| 50 | 12.03 ± 3.41 | 4.57 ± 10.98 | 1.416 ± 0.057 | 0.493 |
| 100 | 7.62 ± 1.83 | 3.70 ± 8.88 | 1.411 ± 0.045 | 0.479 |
| 200 | 4.09 ± 0.76 | 1.23 ± 6.59 | 1.386 ± 0.031 | 0.754 |

The coefficient A becomes smaller as we make the system size larger. This means that the states become more localized in larger system. σ_c also approaches zero as the system size is going to infinity. Energy eigenvalues of states around second peak approach zero in larger system. From these facts, we expect that all states at $E > 0$ localize and there exist isolated extended states only at $E = 0$ in infinite size system with nonzero σ . This is the same situation as in the case of white-noise disorder.

From the above calculations, we can obtain the relation between the correlation length of the random mass λ and the localization length ξ as follows,

$$\xi = C\lambda^\tau, \quad (39)$$

from Eqs.(36) and (38). The value of τ is estimated as around 0.8.

In the random bond XY model, the localization length ξ is related with the correlation length of spins. On the other hand, the impurity density and/or aperiodicity of the positions of impurities control the parameter λ . Therefore we hope that the result (39) can be observed at least qualitatively in the random spin chains.

IV. CONCLUSION

In this paper we studied the random-mass Dirac fermion in one dimension by using the TMM and IVP. In the first half, we explained and verified the validity of the IVP by comparing the obtained results with the analytical calculations. In the second half, we investigated the effects of the nonlocal correlations of the random mass by using Gaussian distribution for distances between jumps of $m(x)$. We obtained relation between the correlation length and localization length. In the subsequent papers [16,17], we shall study the Dirac fermion with long-range correlated random mass.

- [3] A. Comtet, J. Desbois and C. Monthus, *Ann. Phys.* **239**, 312 (1994).
- [4] D. S. Fisher, *Phys. Rev.* **B50**, 3799 (1994); **51**, 707 (1995).
- [5] L. Balents and M. P. A. Fisher, *Phys. Rev.* **B56**, 12970 (1997).
- [6] H. Mathur, *Phys. Rev.* **B56**, 15794 (1997).
- [7] M. Steiner, M. Fabrizio and A. O. Gogolin, *Phys. Rev.* **B57**, 8290 (1998).
- [8] D. G. Shelton and A. M. Tsvelik, *Phys. Rev.* **B57**, 14242 (1998).
- [9] A. O. Gogolin, A. A. Nersesyan, A. M. Tsvelik and Lu Yu, *Nucl. Phys.* **B540**, 705 (1999).
- [10] K. Takeda, T. Tsurumaru, I. Ichinose and M. Kimura, *Nucl. Phys.* **B556**, 545 (1999).
- [11] I. Ichinose and M. Kimura, *Nucl. Phys.* **B554**, 607 (1999).
- [12] I. Ichinose and M. Kimura, *Nucl. Phys.* **B554**, 627 (1999).
- [13] N. Hatano and D. R. Nelson, *Phys. Rev. Lett.* **77**, 570 (1996); *Phys. Rev.* **B56**, 8651 (1997).
- [14] See for example, A. MacKinnon and B. Kramer, *Z. Phys.* **B53**, 1 (1983).
- [15] A. J. Niemi and G. W. Semenoff, *Phys. Rep.* **135**, 99 (1986).
- [16] K. Takeda and I. Ichinose, "Random-mass Dirac fermions in an imaginary vector potential (II): Long-range correlated random mass".
- [17] K. Takeda and I. Ichinose, work in progress.
- [18] G. Theodorou and M. H. Cohen, *Phys. Rev.* **B13**, 4597 (1976).
- [19] T. P. Eggarter and R. Riedinger, *Phys. Rev.* **B18**, 569 (1978).
- [20] Francisco A. B. F. de Moura and Marcelo L. Lyra, *Phys. Rev. Lett.* **81**, 3735 (1998); F. M. Izrailev, A. A. Krokhnin, *Phys. Rev. Lett.* **82**, 4062 (1999).
- [21] B. Huckestein, *Rev. Mod. Phys.* **67**, 357 (1995).

* Electronic address: takeda@icrr.u-tokyo.ac.jp

† Electronic address: ikuo@ks.kyy.nitech.ac.jp

[1] P. W. Anderson, *Phys. Rev.* **109**, 1492 (1958).

[2] A. A. Ovchinnikov and N. S. Erikhman, *Sov. Phys. JETP* **46**, 340 (1977).